



Supplement of

Retrieval of microphysical properties of dust aerosols from extinction, backscattering and depolarization lidar measurements using various particle scattering models

Yuyang Chang et al.

Correspondence to: Qiaoyun Hu (qiaoyun.hu@univ-lille.fr)

The copyright of individual parts of the supplement might differ from the article licence.

Figure S1. Variations of retrieval errors against the true m_R (x-axis) and m_I (rows) when the true r_{eff} is $0.5 \mu\text{m}$ and inverting $(3\beta + 2\alpha + n\delta)$ measurements, which are generated and inverted by the IH model.

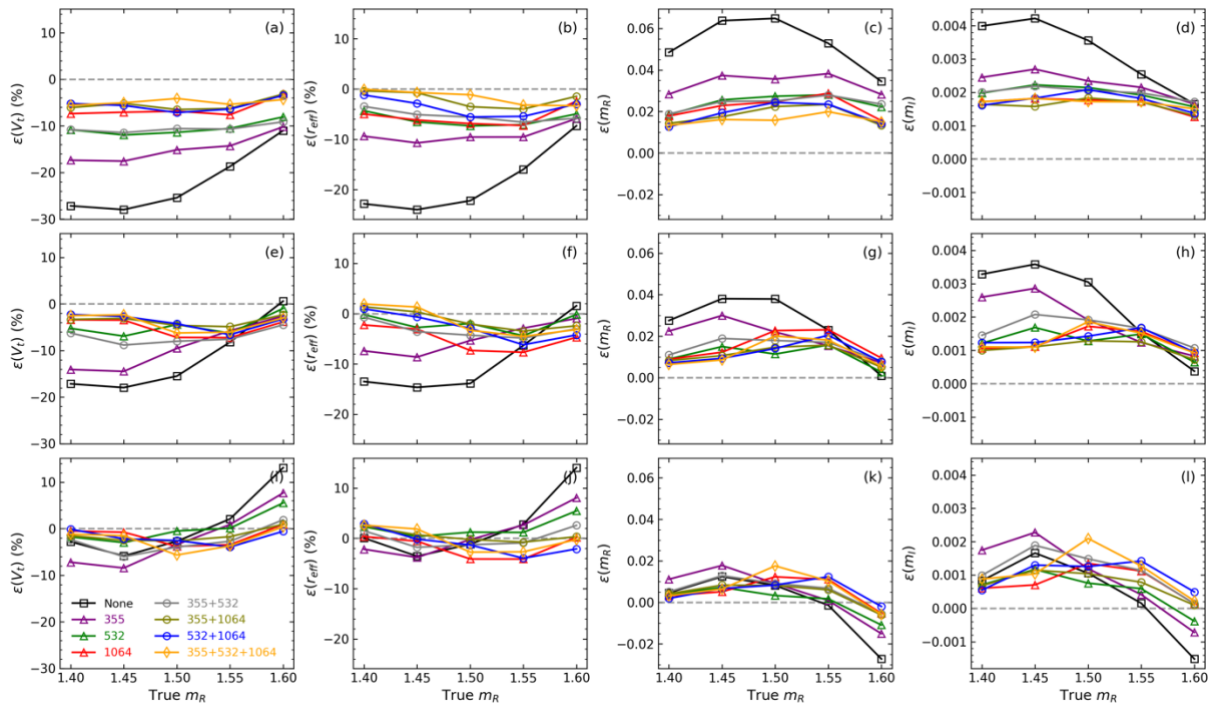


Figure S2. Same as Fig. S1 except that the measurements are generated and inverted by the spheroidal model.

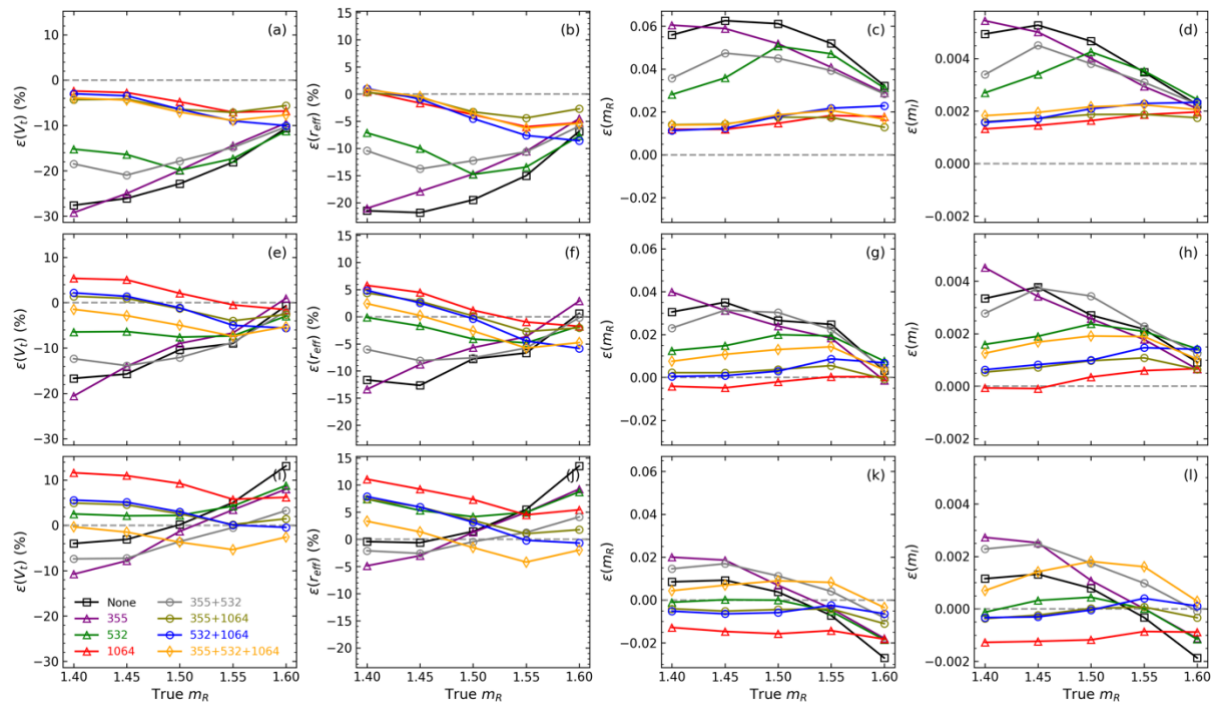


Figure S3. Dust-RGB thermal infrared images from SEVIRI/MSG satellite for the region 30° W-30° E, 15° N-60° N between 14 March 2022, 00:00 UTC and 19 March 2022, 12:00 UTC, provided by EUMETView (https://view.eumetsat.int/productviewer?v=msg_fes:rgb_dust, last access: 18 February 2025). The colors are interpreted as (1) pink: dust aerosols; (2) dark red: thick high ice clouds; (3) black: cirrus clouds; (4) yellow: thick mid-level clouds; (5) green: thin cirrus clouds; (6) cyan and purple: sandy deserts. Note that the colors of deserts can vary considerably depending on surface temperature (e.g., a and b).

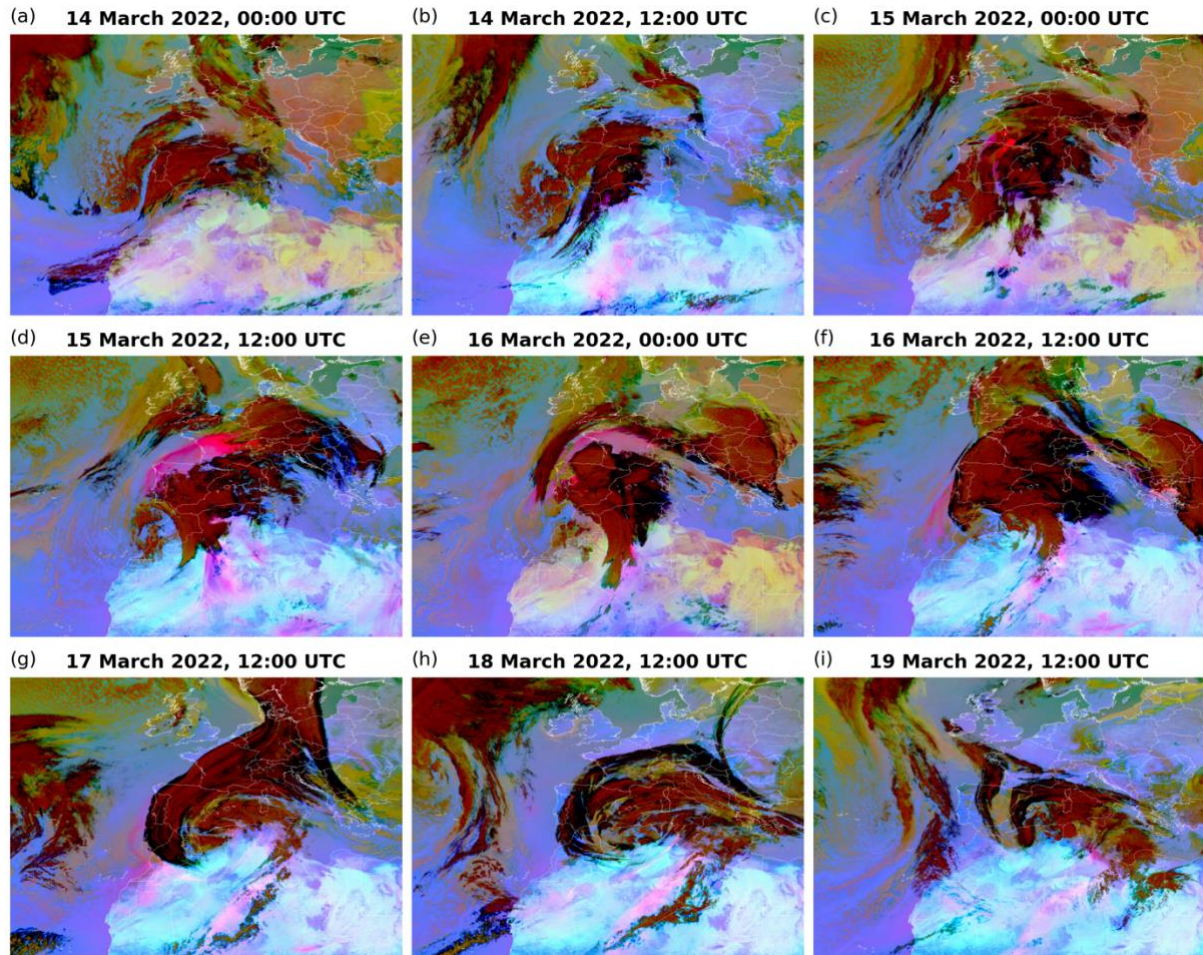


Figure S4. Daily mean sea level pressures (MSLPs) and wind vectors at 10 m for the region 30° W-30° E, 15° N-60° N between 14-19 March 2022. The data are subject to NCEP/DOE Reanalysis II data provided by the NOAA PSL, Boulder, Colorado, USA, from their website at <https://psl.noaa.gov> (last access: 18 February 2025).

